ELECTRO- AND MAGNETOBIOLOGY, 18(3), 257–268 (1999)

CAUSAL STRUCTURE OF THE FRÖHLICH MODEL OF CELLULAR ELECTROMAGNETIC ACTIVITY

Fedor Šrobár* and Jiří Pokorný
Institute of Radio Engineering and Electronics
Czech Academy of Sciences
Praha, Czech Republic

Electromagn Biol Med Downloaded from informahealthcare.com by Universitat de Girona on 12/19/14
For personal use only.

ABSTRACT

The cellular membrane as well as some intracellular structures contain polar macromolecular units, which, especially when receiving energy from such sources as adenosine triphosphate (ATP) decomposition, can perform sustained vibrational motions and hence produce an electromagnetic field. Individual molecular oscillators within groups containing various numbers of them interact with each other and exchange energy with the surroundings. The phenomenon was modeled by H. Fröhlich using a system of coupled nonlinear rate equations for the occupancy numbers of the collective modes of oscillations. This article employs a special diagrammatic technique to represent causal relationships implicit in these equations for the case of two and three individual modes. In this way, better understanding of some known properties (such as energy condensation in the lowest order mode) is achieved, and some new features of the model are uncovered, in particular, the presence and attributes of the feedback loops in the representative diagrams.

INTRODUCTION

Unlike many other constituents of the material world, biologic molecules and subcellular structures lack spatial order. This does not mean, as pointed out by Fröhlich (1), that they cannot exhibit other forms of physical order, such as coherence, that is, macroscopic quantum phase correlations analogous to those existing in lasers. The physics involved in the coherence phenomena may be quite complicated and dependent on the nature of

* To whom correspondence should be addressed. E-mail: srobar@ure.cas.cz

Copyright © 1999 by Marcel Dekker, Inc. www.dekker.com

RIGHTSLINK

the particular system; in the context of this paper we are, generally speaking, concerned with an assembly of polar molecular entities that can interact with each other in both linear and nonlinear manners and can be lifted significantly from thermal equilibrium by an external energy source.

Both the cellular lipid membrane and the cell's interior contain polar macromolecular units. As a consequence, even the thermal vibrations are accompanied by polarization waves and an associated incoherent electromagnetic field. If energy is supplied from intracellular sources such as adenosine triphosphate (ATP) decomposition, these units perform sustained vibrations, giving rise to electromagnetic emission exceeding thermal levels. The neighboring polar units are assumed to be close enough so that there is significant coupling between sizeable groups of oscillators. This, combined with the intrinsic nonlinearity of the system, can lead to coherent structures. In particular, the cytoskeleton is polar, with a large supply of energy, and can satisfy the requirements for emergence of coherent states. Microtubules, cylindrical structures closely associated with the cytoskeleton, are also polar in nature and could support coherent phenomena. In keeping with the thermodynamic laws of open systems, only a portion of the energy supplied to the oscillators is converted into electromagnetic form; ultimately, most of it is passed to the surroundings, which can thus be regarded as a heat bath.

It was H. Fröhlich (2) who put this picture into quantitative (albeit phenomenologic) form. The ensemble of N interacting individual oscillators is equivalent to N collective vibrating modes. These are subject to the laws of quantum mechanics; the time evolution of their occupancy numbers n_i is assumed to be described by a set of nonlinear coupled rate equations ($i, j = 1, 2, \ldots, N$):

$$\frac{dn_i}{dt} = s_i - \Phi_i[n_i \exp(\beta\nu_i) - (n_i + 1)] - \sum_j X_{ij}[n_i(n_j + 1)\exp(\beta\nu_i) - (n_i + 1)n_j \exp(\beta\nu_j)] \quad [1]$$

where s_i and ν_i = pumping rate and frequency of the ith mode, $\beta = h/kT$, and Φ_i and X_{ij} are the linear and nonlinear transition probabilities, respectively; they control the changes in the occupation numbers due to interactions with the heat bath.

Rather than placing emphasis on finding solutions to the Fröhlich equations, we have been trying to bring to light their qualitative properties, namely, the nature of the topologic relationships among basic quantities of the model (3). The principal tool of this analysis is the method of causal diagrams (4), which is a version of the signal flow graph technique. The basic convention of this method associates the diagram $x \rightarrow y$ with the differential relation $\delta y = t_{xy}\delta x$. The change δx of the quantity x is construed as the cause of the change δy of the quantity y; the function t_{xy} [sometimes written as $t(x,y)$] is termed the transmission function of the diagram. Alternatively, δx can be considered as the signal entering the input port x of the diagram; δy is then the output signal available at the port y.

This paper is organized as follows: first we summarize, for easy reference, the results of the preliminary analysis of Fröhlich ensembles comprising two and three coupled oscillators (3), and then we present the results of calculations for several sets of numerical parameters, chosen in such way that they can represent conditions in living cells. Lastly, the results are interpreted and conclusions are drawn.

Electromagn Biol Med Downloaded from informahealthcare.com by Universitat de Girona on 12/19/14
For personal use only.

RIGHTSLINK

DIAGRAMMATIC REPRESENTATION OF THE FRÖHLICH SYSTEMS

In what follows we assume, as in ref. 3, uniform pumping $s_i = s$, and constant coupling coefficients Φ_i and X_{ij}. The latter condition means that the heat bath is so large that the changes in its state due to exchange with the oscillator system are negligible. To facilitate interpretation, we also assume that the transition probabilities are equal, in the sense that $\Phi_i = \Phi$, $X_{ij} = X$ for all i, j. The diagram associated with Eq. [1], appropriate to an ensemble of two coupled oscillators, is shown in Fig. 1a. It contains two oriented paths, $p_1 \equiv ss_1n_1$ (Fig. 1b) and $p_2 \equiv ss_2n_2s_1n_1$ (Fig. 1c), going from the input vertex s to the output vertex n_1 (which means we excite the system at vertex s by injecting a change δs and monitor the result δn_1 of the propagation of this excitation at vertex n_1). There is also one closed path—a feedback loop—present in the diagram, namely, loop $\equiv n_1s_2n_2s_1n_1$ (Fig. 1d). The transmission function for the whole diagram is

$$t_{sn_1} \equiv \frac{\delta n_1}{\delta s} = \frac{t_{p_1} + t_{p_2}}{1 - t_{loop}}. \qquad [2]$$

Figure 2 refers to a system of three Fröhlich oscillators. Note the combinatoric growth in the numbers of significant topologic features: there are now five paths (p_k, k = 1,2, . . .,5) connecting the input port s with the output n_1 (Fig. 3), as well as five feedback loops ($loop_l$, l = 1,2, . . .,5), as shown in Figure 4. The transmission function for the diagram in Figure 2 is

$$t_{sn_1} \equiv \frac{\delta n_1}{\delta s} = \frac{\sum_{k=1}^{5} t_{p_k} - t_{p_1} t_{loop_1}}{1 - \sum_{l=1}^{5} t_{loop_l}} \qquad [3]$$

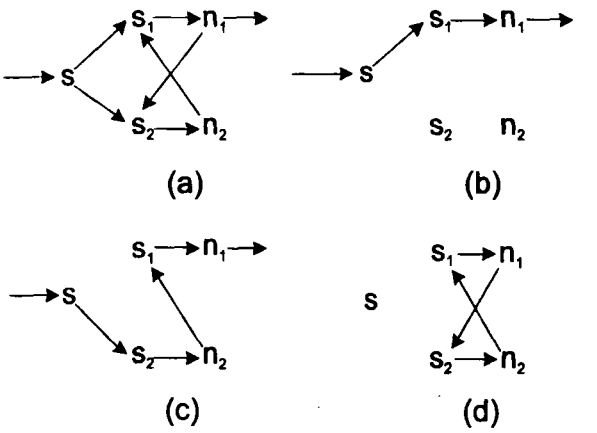


FIGURE 1. Topologic features implicit in the description of a Fröhlich system comprising two oscillators. (a) Diagram corresponding to situation in which response to excitation δs injected at vertex s is monitored at vertex n_1. (b and c) Two oriented paths $p_1 \equiv ss_1n_1$ and $p_2 \equiv ss_2n_2s_1n_1$ connecting the input s with the output n_1. (d) The closed path loop $\equiv n_1s_2n_2s_1n_1$.

Electromagn Biol Med Downloaded from informahealthcare.com by Universitat de Girona on 12/19/14
For personal use only.

RIGHTSLINK

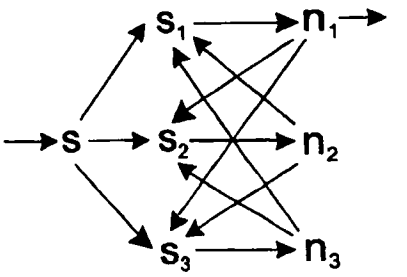


FIGURE 2. Diagram representing the Fröhlich system composed of three oscillators.

Electromagn Biol Med Downloaded from informahealthcare.com by Universitat de Girona on 12/19/14
For personal use only.

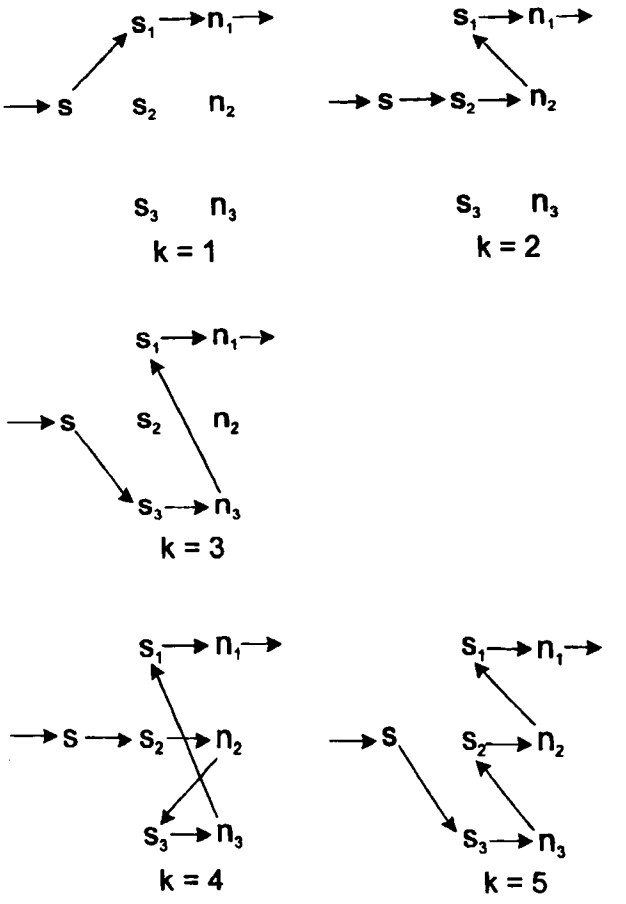


FIGURE 3. The five paths p_k identifiable in the diagram of Figure 2 connecting the input vertex s with the output vertex n_1.

RIGHTSLINK

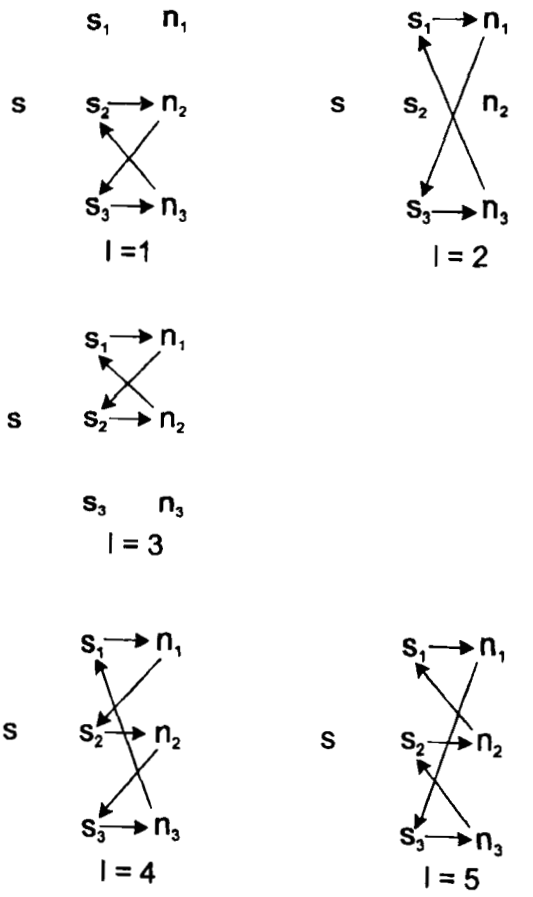


FIGURE 4. The five closed paths of loop_1 contained in the diagram of Figure 2.

The structures of the expressions on the right-hand sides of Eqs. [2] and [3] are similar: the numerator is the transmission function sum of the paths connecting the input with the output [with an additional term $t(p_1)t(\text{loop}_1)$ in Eq. [3]], while the denominator is one minus the sum of the transmission functions of the feedback loops.

To give the reader a feeling for the computations involved, we point out that the transmission functions of (open or closed) diagram paths are the product of the transmission functions of the elementary diagrams (diagram edges) composing it, e.g.,

$$t_{p_3} = t_{ss_3} t_{s_3 n_3} t_{n_3 s_1} t_{s_1 n_1}. \qquad [4]$$

Again, as an example, the transmission function of the edge $s_1 n_1$ is given by the expression

$$\frac{1}{t_{s_1 n_1}} = \Phi(e^{\beta\nu_1} - 1) + X[(e^{\beta\nu_1} - e^{\beta\nu_2})n_2 + (e^{\beta\nu_1} - e^{\beta\nu_3})n_3 + 2e^{\beta\nu_1}]. \qquad [5]$$

(Both examples refer to the case of three oscillators.)

Electromagn Biol Med Downloaded from informahealthcare.com by Universitat de Girona on 12/19/14
For personal use only.

RIGHTSLINK

NUMERICAL STUDY

The mathematical apparatus outlined in the previous section has been employed to evaluate the behavior of Fröhlich ensembles consisting of two and three oscillators. We denote as ν_1 the frequency of the lowest energy (fundamental) oscillator mode; higher order modes are numbered in such way that $\nu_1 < \nu_2$ (for two oscillators) or $\nu_1 < \nu_2 < \nu_3$ (for three oscillators). With a view to biophysical reality, as well as to our own attempts aimed at detecting the electromagnetic activity of living cells (5), we have selected the following three frequency ranges: 0.1–1 THz (1 THz = 10^{12} Hz), 0.01–0.1 THz, and 1–10 GHz. As to the values of the coefficients Φ and X, we have chosen the cases of weak (Φ = 0.01 s^{-1}, X = 0.001 s^{-1}) and strong (Φ = 1 s^{-1}, X = 0.1 s^{-1}) coupling with the heat bath. The relevant literature provides very few clues as to the choice of the coupling coefficients. The two selected values of X bracket the value of 0.04 estimated by Chatterjee *et al.* (6). The values of ϕ were chosen on the rationale that linear transition probabilities are likely to be larger than the nonlinear ones. (In the reality of the cell, the magnitude of coupling may be a function of the degree of protein phosphorylation that enhances Coulomb forces.)

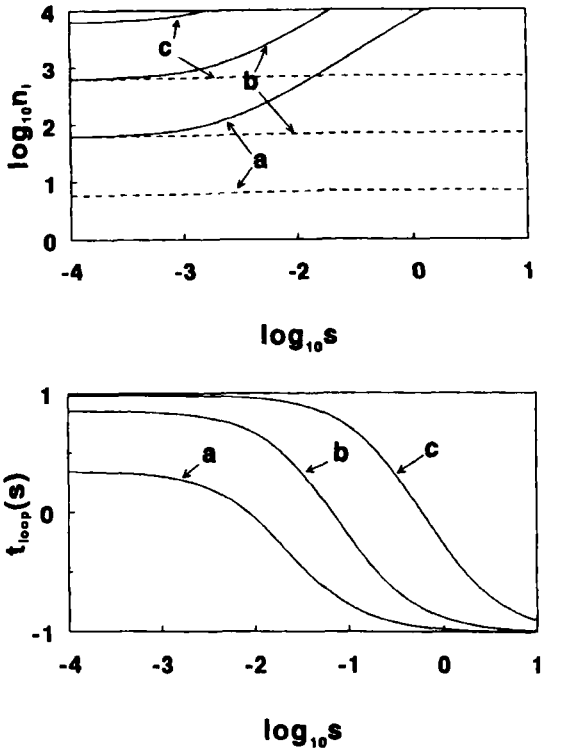


FIGURE 5. Dependencies of the occupancy numbers (upper panel) and transmission functions of the feedback loop (lower panel) on the pumping rate for the case of two oscillators. In the upper panel, solid lines refer to n_1 and broken lines to n_2. Frequency values: ν_1 = 0.1 THz, ν_2 = 1 THZ (curves labeled a), ν_1 = 0.01 THz, ν_2 = 0.1 THz (b), ν_1 = 1 GHz, ν_2 = 10 GHz (c). Weak coupling with the heat bath: Φ = 0.01 s^{-1}, X = 0.001 s^{-1}.

Electromagn Biol Med Downloaded from informahealthcare.com by Universitat de Girona on 12/19/14
For personal use only.

RIGHTSLINK

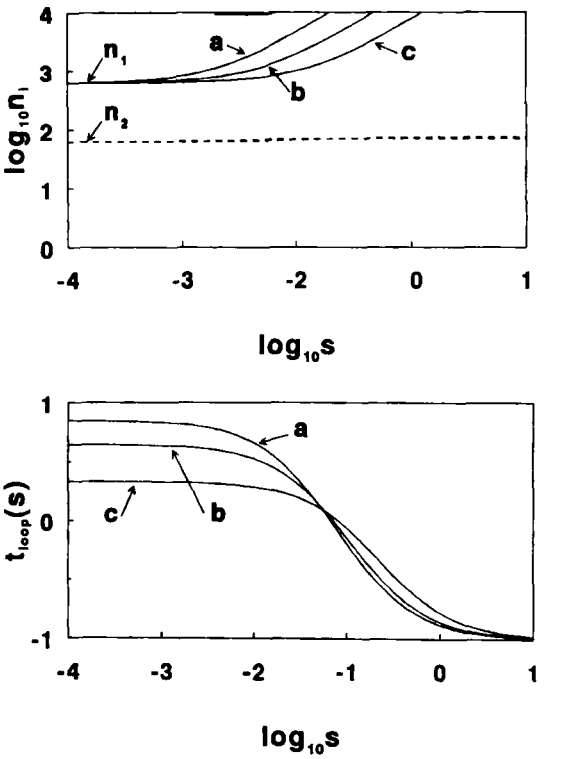


FIGURE 6. Similar dependencies as in Figure 5 with frequency values fixed (ν_1 = 0.01 THz, ν_2 = 0.1 THz) and the ratio of linear to nonlinear coupling coefficients Φ/X varied from 10 (curves labeled (a) to 30 (b) to 100 (c). Reference value X = 0.001 s^{-1} in all cases.

Starting with a two-oscillator ensemble, Figure 5 presents the dependencies of the occupancy numbers (upper panel) and transmission functions (lower panel) on the pumping rate for the three frequency ranges and for weak coupling with the heat bath. (The numerical values of the parameters relevant for this figure, as well as for the following figures, are specified in the respective captions.) The effect of varying the ratio of the linear to the nonlinear transition probabilities on one of these dependencies is illustrated in Figure 6. A case of strong coupling is shown in Figure 7. Figure 8 demonstrates how the transmission functions of the paths connecting the "pumping vertex" s with the "population vertices" n_1 and n_2 vary with the pumping level s.

The system comprising three oscillators was found to behave in many (but not all) ways similarly to that of two oscillators; we have selected dependencies presented in Figure 9 and 10 to represent this group.

DISCUSSION AND CONCLUSIONS

The curves in the upper panels of Figures 5, 6, 7, and 9 exhibit the well-known feature of Fröhlich systems, namely, the condensation of energy into the lowest energy (fundamental) mode. The present analysis offers an insight into the mechanisms behind

Electromagn Biol Med Downloaded from informahealthcare.com by Universitat de Girona on 12/19/14
For personal use only.

RIGHTSLINK

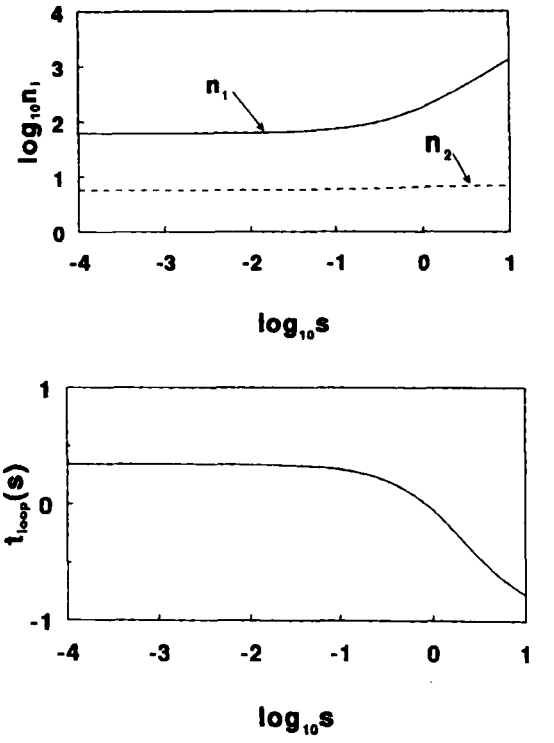


FIGURE 7. The effect of strong coupling (Φ = 1 s^{-1}, X = 0.1 s^{-1}) on the dependencies labelled a (ν_1 = 0.1 THz, ν_2 = 1 THz) in Figure 5.

this phenomenon: In Figure 8 we can see that while the magnitude of the transmission functions of the channels $p_1 \equiv ss_1n_1$ and $p_2 \equiv ss_2n_2s_1n_1$ connecting the pumping vertex s with the vertex representing population of the fundamental mode n_1 increase with rising pumping level s (upper panel), the reverse is observed for the transmission functions of the channels ss_2n_2 and $ss_1n_1s_2n_2$ that feed signal to the vertex n_2 (lower panel). Actually, at higher pumping levels, the latter transmission functions tend to asymptotically approach zero. More important still, as one can note by comparing vertical scales on both charts of Figure 8, the transmission functions of the paths feeding vertex n_1 are higher by a factor of about 1000 than those feeding vertex n_2. The situation for the case of three oscillators is analogous—the population n_1 of the fundamental mode has preferential access to feeding signals originating from the pumping port s, while the higher order mode populations n_2 and n_3 are discriminated against in this respect.

Other features apparent in the upper panels of Figures 5, 6, 7, and 9 have been understood without recourse to diagrammatical technique: the population curves are shifted upward with decreasing oscillator frequencies (as we proceed from label a to b to c in the upper panel of Fig. 5). This is due to increase in the thermal equilibrium occupancy of the oscillators. Comparing curves labeled a in Figure 5 (weak coupling) with dependencies traced in Figure 7 (strong coupling) shows that increased coupling to the heat bath shifts the n_i versus s curves to the right. Higher pumping is required to

Electromagn Biol Med Downloaded from informahealthcare.com by Universitat de Girona on 12/19/14
For personal use only.

RIGHTSLINK

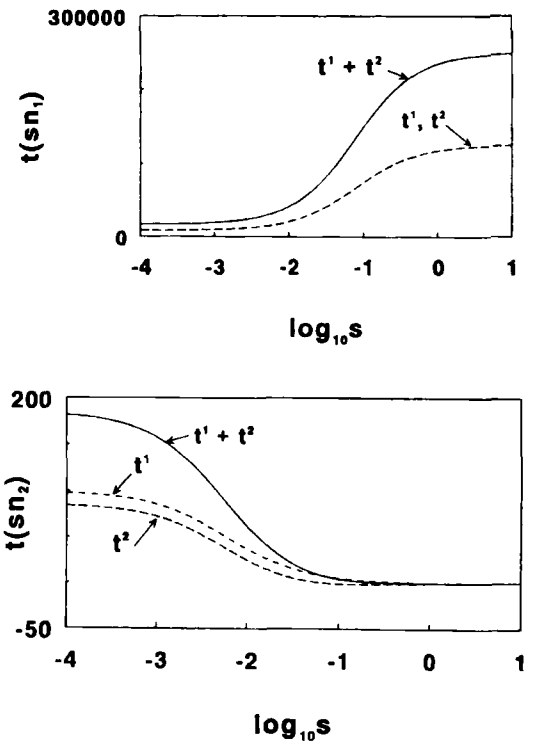


FIGURE 8. Dependencies of the transmission functions of the paths connecting the input vertex s with the output vertex s_1 (upper panel) or n_2 (lower panel) on the pumping rate. Also shown are the sums of the transmission functions of the two parallel paths. Two oscillators are given, ν_1 = 0.01 THz, ν_2 = 0.1 THz, with weak coupling.

achieve the same increase in population when more energy is given off to the surroundings. Again, these trends are repeated in the case of three oscillators.

Increasing the role of the nonlinear processes (i.e., progressing from curves labeled c to those labeled b to those labeled a) is seen in Figure 6 to lead to easier condensation of energy in the fundamental mode. The higher energy mode population level is indifferent to this change.

A salient feature of the diagrams in Figures 1a and 2 is the presence of a feedback loop or loops. The presence of such elements in the system's topology is a necessary condition for the occurrence of bistable behavior; the sufficient condition requires that the sum of the transmission functions of all feedback loops cross the critical level of unity in two distinct states (4).

As can be seen from Figures 5, 6, 7, and 9, there is no indication in our results that the sufficient condition can be met in the Fröhlich systems considered. The sum of the transmission functions approaches the critical level of unity asymptotically at decreasing pumping levels, $\lim_{s\to 0} t_{loop} = 1$, but it definitely remains below it. Comparing the changes connected with transition from a system of two to a system of three oscillators, there is a strong suggestion that the latter statement remains true for ensembles encompassing

Electromagn Biol Med Downloaded from informahealthcare.com by Universitat de Girona on 12/19/14
For personal use only.

RIGHTSLINK

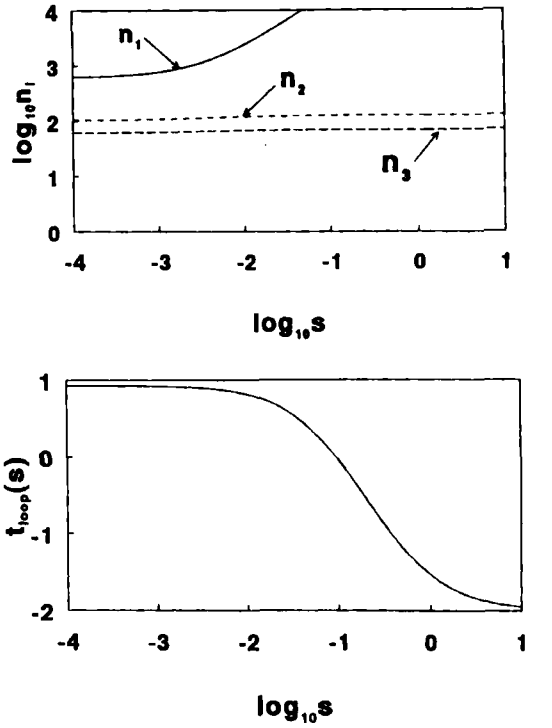


FIGURE 9. Dependencies of the occupancy numbers (upper panel) and of the sum of the transmission functions of the five feedback loops (lower panel) on the pumping rate for the case of three oscillators. Frequency values are $\nu_1 = 0.01$ THz, $\nu_2 = 0.06$ THz, $\nu_3 = 0.1$ THz, with weak coupling.

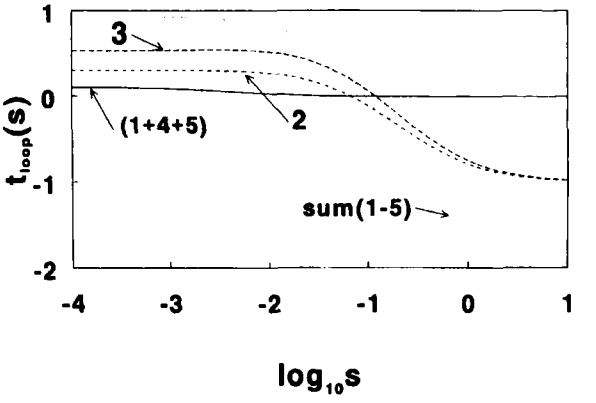


FIGURE 10. Dependencies of the transmission functions of the individual feedback loops and their sum on the pumping rate for the system of three oscillators depicted in Figure 10. The curves are labeled with the loop number l; transmission functions of loops 1, 4, and 5 are grouped together because each of them is quite small when compared with the transmission function of either $loop_2$ or $loop_3$.

Electromagn Biol Med Downloaded from informahealthcare.com by Universitat de Girona on 12/19/14
For personal use only.

RIGHTSLINK

more than three oscillators. Accordingly, one cannot expect bistable behavior in Fröhlich systems, even in those with more than two oscillators, notwithstanding the presence of many feedback loops in the diagrams representing the rate equations.

There is, however, a significant trait in the t_{loop} versus s dependencies shown in the lower panels of Figures 5, 6, 7, and 9. All of them roll off monotonically and smoothly between two asymptotic levels: The upper one, approached for small pumping values by both the two- and three-oscillator systems, equals plus one. The lower one, approached for high pumping levels, equals minus one for the two-oscillator system and minus two for the three-oscillator system. The fact that the range of variation is bounded in this way and that both limiting values are integers is quite amazing, given the behavior of many other physical systems we have been analyzing so far (e.g., refs. 4 and 7).

Figure 10 shows the predominance of the transmission functions of two of the feedback loops ($loop_2$ and $loop_3$) in the overall sum. Inspection of Figure 4 suggests an explanation for this. Loops with labels $l = 1$, 2, and 3, involving vertices pertaining to only two oscillators each, are topologically simpler than the remaining two, which involve vertices representing all three oscillators; one can expect their contribution to be greater. However, one of them, $loop_1$, does not contain vertex n_1, which is the one at which the output signal is monitored. This leaves $loop_2$ and $loop_3$ as dominant contributors to the sum.

In summary, diagrammatical analysis has been used to gain better insight into some known properties of the Fröhlich model (such as the energy condensation in the fundamental mode) and to bring to light some new features: the topologic structure of the mutual relationships among the main quantities together with the presence and properties of the feedback loops in the causal patterns. Even though there may be an abundance of feedback loops for systems with higher numbers of oscillators, our study tends to eliminate the possibility of the occurrence of bistable states in Fröhlich systems. On the other hand, the issue of feedback loops is highly relevant to such important topics as stability of oscillatory regimes, noise generation, or synthesis of an equivalent electronic circuit of the biologic cell to assist in design of measurement apparatus and interpretation of the experimental results.

Given the important position the Fröhlich model has in the theory of electromagnetic manifestations of living cells, the findings presented in this paper may contribute to the further development of the field. The diagrammatic method has not been introduced to emulate the traditional analytic tools in solving the Fröhlich rate equations; its main strength is to visualize the causal relationships implicit in the physical models and to provide qualitative formalism for evaluating them.

Electromagn Biol Med Downloaded from informahealthcare.com by Universitat de Girona on 12/19/14
For personal use only.

ACKNOWLEDGMENTS

Support of the Grant Agency of the Czech Republic (project no. 102/97/0867) is gratefully acknowledged.

REFERENCES

1. Fröhlich, H.: Long-range coherence in biological systems, Nuovo Cimento *7*, 399–418, 1977.

RIGHTSLINK

2. Fröhlich, H.: Quantum mechanical concepts in biology, in *Theoretical Physics and Biology*, M. Maurois, ed., North Holland, Amsterdam, 13–22, 1969.
3. Šrobár, F. and Pokorný, J.: Topology of mutual relationships implicit in the Fröhlich model, Bioelectrochem Bioenerg *41*, 31–33, 1996.
4. Šrobár, F.: Feedback relationships—a neglected theme in physics, Eur. J. Phys. *13*, 1–8, 1992.
5. Jelínek, F., Šaroch, J., Trkal, V., and Pokorný, J.: Measurement system for experimental verification of Fröhlich electromagnetic field, Bioelectrochem Bioenerg *41*, 35–38, 1996.
6. Chatterjee, R., Tuszyński J.A., and Paul, R.: Comments on the Bose condensation of phonons in the biological systems, Int. J. Quantum Chem. *23*, 709–712, 1983.
7. Šrobár, F.: Feedback relationships and threshold current in semiconductor injection lasers, Optical Quantum Electron. *25*, 27–35, 1993.

Electromagn Biol Med Downloaded from informahealthcare.com by Universitat de Girona on 12/19/14
For personal use only.

RIGHTSLINK